Ring Closure Mediated by Intramolecular Hydrogen Transfer in the Decomposition of a Push−Pull Nitroaromatic: TATB

Christine J. Wu* and Laurence E. Fried

Lawrence Livermore National Laboratory, University of California, Livermore, California 94551

Received: March 17, 2000

Using gradient-corrected density functional theory, we have investigated various competing mechanisms involved in the early stages of the decomposition of a "push−pull" (containing both electron-donating and -withdrawing groups) aromatic (1,3,5-triamino-2,4,6-trinitrobeznene, TATB), and particularly how hydrogen transfer affects the competition between ring closure and single bond scission. On the basis of the obtained energetics, we found several previously suggested mechanisms to be energetically disfavored. These mechanisms include direct N−H, N−O, C−NH_2 bond dissociation, carbon ring cleavage, and the production of NO_2^{-1} anion. Our results indicate that the rate-limiting step is ring closure mediated by intramolecular hydrogen transfer. This mechanism is predicted to have a barrier height of 47.5 kcal/mol. The hydrogen motion forms a biradical state which we suggest is the precursor to further decomposition products, such as benzofurazans.

I. Introduction

Benzene rings with push−pull substituents have been previously investigated for the underlying forces that determine their molecular structures. Baldridge and Siegel used the concept of static "gear clashing" (steric effects) in combination with the push−pull effect to explain why some push−pull benzenes are planar, while others are not.[1] One push−pull nitroaromatic whose structure is still a subject of debate is TATB ($C_6H_6O_6N_6$). In contrast to previous reports, Baldridge and Siegel predicted that TATB is not completely flat.[1]

Although determining the structures of push−pull nitroaromatics is of scientific importance, a more intriguing question is the nature of decomposition chemistry in push−pull nitroaromatics. The dominant thermal decomposition pathway for simple substituted benzenes is often unimolecular bond fission. A good example is C−NO_2 bond fission in nitrobenzene.[2,3]

In push−pull aromatics where amino and nitro groups are ortho to one another, the formation of heterocyclic rings can compete with simple bond fission. The overall energetics for such a reaction are particularly favorable with the nitro and amino groups, since the reaction pathway then involves the formation of water. We chose TATB to be our model system for both scientific and technological reasons. First, it has a strong hydrogen-bonding network, and thus it provides us an ideal system to study how hydrogen bonding affects the chemistry of these nitroaromatics. Second, TATB is a well-known energetic material. Thus, the kinetics of TATB decomposition is of importance to the defense and chemical industries. New understanding not only gives insight into the chemistry of other energetic compounds, but also to related chemicals, such as dyes in which ring closure mechanisms may play a role in their stabilities.

There is a great need for theory to play a role in determining the kinetics of TATB decomposition. In comparison to gas phase combustion, the chemical processes involved in the decomposition of solid TATB are still poorly understood. This lack of understanding is partially due to the experimental difficulties encountered in probing reaction intermediates in the solid state. Therefore, it is very useful for us to study the decomposition of the gas phase TATB molecule. The energetics of gas phase decomposition pathways provide insight regarding possible pathways in solid phase decomposition. It is important to note, however, that condensed phase decomposition mechanisms often differ from those in the gas phase.

It is not fully understood why TATB is insensitive to external stimuli.[4] However, it is believed that endothermic decomposition processes play an important role in the initiation reactions of energetic compounds. Arrhenius fits to the overall decomposition kinetics of TATB have been made to several experiments. The reported values for the activation energy are scattered between 40 and 60 kcal/mol.[5−8] The lower value has been suggested to be the result of molecular sublimation.[8] Although the details of the decomposition mechanism continue to be a subject of debate, what has been repeatedly observed is the loss of nitro group (NO_2) as the primary event in the initial stages of TATB decomposition.[9−12]

There are two previously suggested reaction pathways which contribute to the loss of nitro group: (1) removal of NO_2 from the benzene ring,[10] and (2) the formation of benzofuroxan and benzofurazan derivatives.[11] Benzofurazan formation is thought to occur through the abstraction of water via a ring closure path.[11,12] However, the detailed chemical sequence of the events is unknown. The suggestion of C−NO_2 bond dissociation is primarily based on the qualitative observation that C−NO_2 is generally a much weaker bond than C−NH_2. To the best of our knowledge, the C−NO_2 bond strength of TATB has not been measured experimentally or calculated by high-level theory. An accurate prediction of the C−NO_2 bond strength is therefore important since its value in comparison to the overall activation barrier allows us to estimate the probability of this path.

The ring closure path which forms benzofuroxan and its derivatives has been a subject of conflicting experimental evidence.[11−15] For instance, it is strongly supported by Sharma et. al[11,12] Using XPS, chromatography (TLC), and mass

10.1021/jp001019r CCC: $19.00
Published on Web 06/16/2000

spectroscopy, they found the presence of benzofurazan compounds in the molecular decomposition of TATB by different stimuli, such as heat, electron beams, UV photolysis, and impact.[11,12] Land et. al have also observed mono-, bis-, and trisbenzofurazan products in the thermal decomposition of TATB using simultaneous thermogravimetric modulated beam mass spectrometry.[13] However, no spectral features of these molecules were observed by Catalano and Rolon using infrared (IR) spectra.[14] They also found little water among decomposition products.[15] Therefore, they discounted the importance of benzofuroxan and benzofurazan formation in TATB decomposition.

Besides $C-NO_2$ bond rupture, there are other two mechanisms involving simple bond scission that have been proposed for TATB decomposition. Despite the general belief that $C-NH_2$ is a stronger bond than $C-NO_2$, Makashir and Kurian suggested that the primary step in the thermal decomposition of TATB is loss of the amino group.[16] This is based on their observation that the relative IR intensity of the $C-NH_2$ bond stretching mode drops faster than that of the $C-NO_2$ symmetric stretching mode during TATB decomposition. They argued that the interaction between $C-NH_2$ and $C-NO_2$ leads to a weakening of the $C-NH_2$ bond. Another proposed pathway involves loss of oxygen atom.[17] Using time-of-flight mass spectroscopy, Ostmark detected fragment of $C_6H_6O_5N_6$ which has a *m*/*z* peak at 248 during shock-induced initiation of TATB. Therefore, he concluded that the conversion of a nitro group to a nitroso group occurs during TATB decomposition.[17]

A carbon ring cleavage mechanism has also been suggested previously by Farber and Srivastava.[18] In their thermal decomposition experiments, they observed a nearly equal intensity of amu 144 and 114 peaks in the mass spectra of decomposition products,[18] which correspond to the two fragment products of the ring cleavage. They also made a rough estimate of the activation energy barrier of 43 kcal/mol from the variation of intensity of the amu 114 species with increasing temperature, which is considerably smaller than other reported values.[8]

The role of hydrogen in the decomposition of TATB has been studied by Rogers, Janney, and Ebinger.[7] Their isotopic kinetics data indicate that motion of the hydrogens is involved in the earlier stages of TATB decomposition. One possible explanation of such a motion is homolytic N−H bond fission. Davis and Brower[19] proposed an alternative mechanism involving intermolecular hydrogen transfer. They suggested that the dominant activation process is hydrogen moving from the nitrogen atom of an amino group to the adjacent oxygen atom of the nitro group.[19] This type of mechanism was identified in the decompositions of other aromatic nitro compounds (e.g., nitrobenzene) in aromatic solvents.[20] In the present paper we propose an intramolecular hydrogen transfer mechanism, where the hydrogen of an amino group moves to the nearest-neighbor oxygen atom of a nitro group in the same TATB molecule.

Previous ab initio studies of TATB have been focused on its molecular structure, rather than its decomposition.[1] In the present work, we have investigated the decomposition mechanisms of TATB using gradient-corrected density functional theory (DFT). Studied pathways include (1) homolytic bond dissociation involving $C-NO_2$, N−O and N−H and $C-NH_2$ (shown in Figure 1a−d); (2) formation of ions in $C-NO_2$ bond dissociation; (shown in Figure 1e); (3) carbon ring cleavage (shown in Figure 1f); (4) both intra- and intermolecular hydrogen transfers (shown in Figure 2); and (5) ring closure forming benzofurazan and benzofuroxan derivatives (shown in Figure 3). On the basis of our calculations, we propose that the ring closure pathway mediated by the biradical state formed after intramolecular hydrogen transfer dominates the kinetics of the early stages of TATB decomposition.

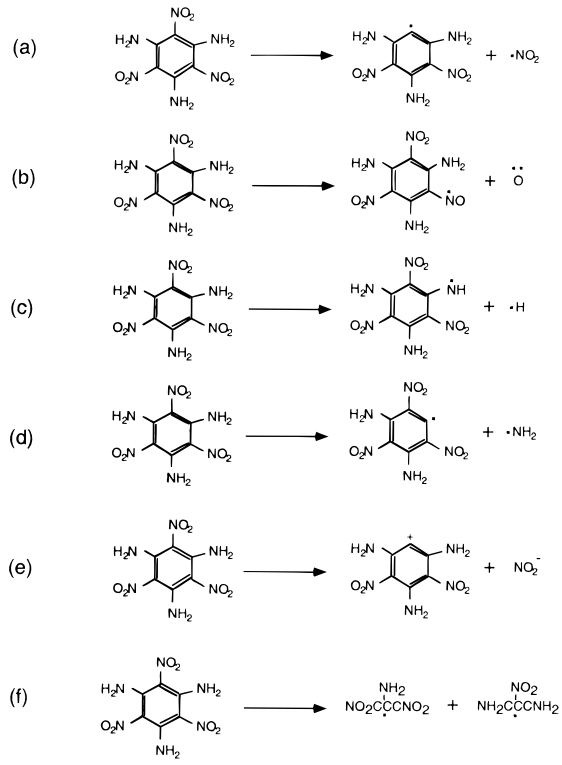

Figure 1. Reaction pathways for TATB: (a) $C-NO_2$, (b) N−O, (c) N−H, (d) $C-NH_2$ bonds of TATB, (e) formation of NO_2^{-1}, and (f) the carbon ring cleavage pathway.

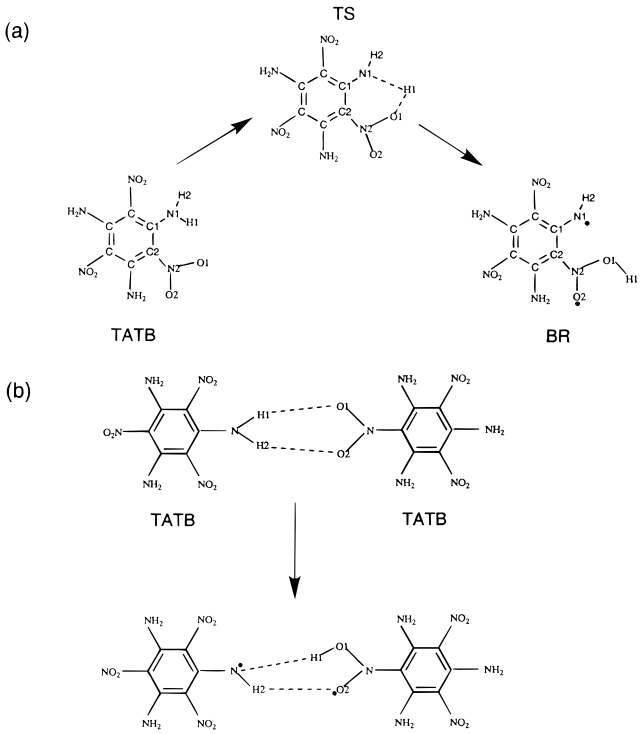

Figure 2. Schematic drawings of hydrogen transfer via (a) the intramolecular and (b) the intermolecular pathway.

II. Computational Details

DFT with gradient-corrected functionals has been proven to be a cost-effective and reliable procedure for calculating

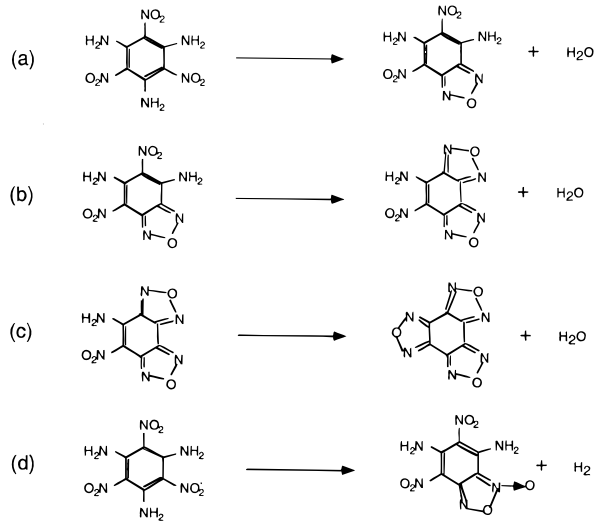

Figure 3. Schematic drawings of the formation of (a) monobenzofurazan, (b) disbenzofurazan, (c) trisbenzofurazan, and (d) benzofuroxan.

atomization energies, reaction energies, and barrier heights.[21−23] For instance, using a numerical basis set, Becke reported an average deviation of less than 4 kcal/mol between DFT and experimental atomization energy.[21] Durant tested the performance of several common functionals in barrier heights and reported an error bar of less than 6 kcal/mol.[23] He also concluded that those functionals perform reasonably well in predicting geometries and vibrational frequencies.[23]

In this work, we carried out total energy calculations using the Gaussian 94[24] package with spin-polarized gradient-corrected exchange and correlation functionals. The procedures are based on the spin-unrestricted Kohn−Sham[25] formalism. We have chosen the gradient-corrected BPW91 functional; B and PW91 refer to the Becke's 1988 exchange functional[26] and the Perdew−Wang's correlation functional, respectively.[27] We have tested three other functionals B3LYP, BLYP, and B3PW91 in a recent study of RDX dissociation,[28] but found no significant difference between them.

Three Gaussian-type basis sets were used for the Kohn−Sham orbital expansion: Dunning's valence double-ζ (D95V),[29] Dunning's more recent correlation consistent polarized valence double-ζ basis sets (cc-pVDZ),[30] and cc-pVDZ plus a diffuse function (Aug-cc-pVDZ). We used the synchronous transit-guided quasi-Newton method in transition state searches. Harmonic vibrational frequency calculations were carried out only with D95V basis set, which also gives us the zero-point vibrational energy corrections.

III. Results and Discussion

A. Molecular Structure of TATB. According to the report of Baldridge and Siegel,[1] the gas phase minimum energy geometry of TATB is not planar. The geometry that they obtained has a planar carbon ring with the amino and nitro groups rotated out of the plane. However, the predicted torsion angles for the amino and nitro groups are significantly different depending on their choice of method. For instance, Hartree−Fock (HF) with the 6-31G(d) basis set gives large torsional angles of 8° (amino)/25° (nitro), while LDA with a double numerical basis set augmented by polarization predicts only 3° (amino)/6° (nitro).

In agreement with Baldridge and Siegel, we also found that the out-of-plane angle of an amino and nitro group is sensitive to the choice of methods. In Table 1, we list the torsion angles of amino and nitro groups obtained by HF, LDA, and BPW91 calculations using various basis sets. Using the same level of theory (HF/6-31G(d)), we obtained torsion angles of 9° (amino)/28° (nitro) similar to 8° (amino)/25° (nitro) of Baldridge and Siegel. The 1°−3° differences in values are perhaps due to the large error bars associated with locating a minimum of a shallow potential energy well. We also observed a reduction of the out-of-plane torsional angles when we switched from HF to LDA. This is not surprising since HF does not include electron correlation and thus cannot describe hydrogen-bonding properly.

TABLE 1: Torsion Angle (in deg) of the Amino (∠HNCC) and Nitro (∠ONCC) Groups out of the Carbon Ring, and the Nearest-Neighbor Distance between the Amino Group H and the Nitro Group O, *R*(H−O) (in Å)

method/basis set	∠HNCC	∠ONCC	*R*(H−O)
HF/D95V	−8.0	+18.9	1.797
HF/6-31G(d)	−9.3	+28.1	1.857
HF/cc-pvdz	−8.9	+26.2	1.834
LDA/D95V	−1.5	+1.9	1.630
LDA/cc-pvdz	−0.1	+0.3	1.599
LDA/Aug-cc-pvdz	0.0	+0.0	1.613
BPW91/D95V	−1.1	+1.5	1.691
BPW91/cc-pvdz	−1.1	+1.5	1.692
BPW91/Aug-cc-pvdz	−0.1	+0.2	1.677

In addition, we found that the angles are sensitive to the basis set size as well. Note that an increase in the basis set size gives a significant change in the relative values of angles. For instance, once we increase the size of basis set to Aug-cc-pVDZ, the rotation angles nearly vanish in both LDA and BPW91 calculations. Because of computational cost, we have not evaluated harmonic frequencies with the Aug-cc-pVDZ basis set. Calculations with other basis sets were verified to be true minima on the basis of frequency calculations.

The description of hydrogen bonding is the critical element in predicting TATB geometry. Electron conjugation between the aromatic benzene ring and the functional groups favors a planar structure. The torsional angle of the functional groups also depends on the preferred hydrogen bond distance. For instance, as shown in Table 1, HF predicts a longer H−O hydrogen bond than both LDA and BPW91; thus, it gives a nonplanar minimum configuration in which amino and nitro groups have to rotate out of the plane to compensate for a longer bond. Both conjugation and hydrogen bonding require a large basis set since they are not localized phenomena. Thus, we conclude that the previously predicted out-of-plane rotation of amino and nitro groups are likely due to the inadequate basis set. The minimum energy structure of TATB is essentially planar, although it is easy to rotate amino and the nitro groups a few degrees of out of the plane at the room temperature since the potential energy surface in this direction is fairly flat.

The various bond lengths of TATB optimized by DFT/BPW91 using D95V, cc-pVDZ, and Aug-cc-pVDZ basis sets are listed in Table 2. The calculated geometry agrees well with the previously reported X-ray crystallography of TATB except N−H bonds.[31] The X-ray data indicates N−H bond distances of 0.86, 0.89, 0.80, 0.89, 1.05, and 1.06 Å. The values of 1.05 and 1.06 Å agree well with our result of 1.03 Å. We note that the experimental N−H bond distances of less than 0.9 Å are unusually short and also are in disagreement with plane wave DFT calculations of crystalline TATB.[32] This disagreement is not surprising since X-ray scattering is not a reliable method for determining positions of hydrogen.

B. Bond Dissociation Energies of Functional Groups. The energetic cost of removing functional groups from TATB were

TABLE 2: Calculated DFT/BPW91 Bond Lengths (Å) of TATB from D95V, cc-pvdz, and Aug-cc-pvdz Basis Sets

bond	D95V	cc-pvdz	Aug-cc-pvdz	experiment[a]
C−C	1.444	1.451	1.452	1.441
C−N (nitro)	1.419	1.441	1.436	1.422
C−N (amino)	1.338	1.334	1.334	1.316
N−O	1.298	1.259	1.262	1.243
N−H	1.045	1.033	1.029	0.925[a]

[a] Taken from ref 31, where 0.925 is averaged from reported N−H bond lengths of 0.86,0.89,0.80,0.89,1.05, and 1.06.

TABLE 3: DFT/BPW91 Reaction Energies (kcal/mol) for Breaking C−NO_2, N−O, N−H, and C−NH_2 Bonds of TATB, Forming NO_2^{-1} Ion and Carbon Ring Cleavage Pathway[a]

reaction/basis set	D95V	cc-pVDZ	Aug-cc-pVDZ
$C_6H_6O_6N_6 \rightarrow C_6H_6O_4N_5 + NO_2$	77.2	73.9	68.5(63.9)
$C_6H_6O_6N_6 \rightarrow C_6H_6O_5N_6 + O$	76.0	93.1	89.5(86.8)
$C_6H_6O_6N_6 \rightarrow C_6H_5O_6N_6 + H$	120.0	109.0	107.8(96.3)
$C_6H_6O_6N_6 \rightarrow C_6H_4O_6N_5 + NH_2$	124.1	117.5	111.0(103.4)
$C_6H_6O_6N_6 \rightarrow C_6H_6O_4N_5^{+1} + NO_2^{-1}$	226.5	234.6	208.8
$C_6H_6O_6N_6 \rightarrow C_3N_3O_2H_4 + C_3N_3O_4H_2$	209.3	203.0	192.7(185.8)

[a] Numbers in parentheses include the zero-point energy correction.

computed using DFT with the BPW91 functional. The results are listed in Table 3 for various basis sets. The zero-point energy corrections were calculated at the BPW91/D95V level. Our best estimates (at the BPW91/Aug-cc-pVDZ level) of dissociation energies for C−NO_2, N−O, N−H, and C−NH_2 bonds are 63.9, 86.8, 96.3, and 103.4 kcal/mol, respectively. Note that increasing the size of the basis set from D95V to Aug-cc-pVDZ systematically lowers the bond energies of C−NO_2, C−NH_2, and N−H. The trend is in the opposite direction for the N−O bond energy. The N−O bond dissociation pathway is spin forbidden, due to the formation of atomic oxygen in its triplet state.

As shown in Table 3, C−NO_2 has the lowest homolytic bond dissociation energy. We have assumed that the barrier for C−NO_2 bond fission is the same as its bond strength, since the barrier for the backward recombination reaction is typically negligible for most spin-allowed homolytic bond-breaking processes. The calculated bond dissociation energy of 63.9 kcal/mol is within the upper end of the reported overall TATB decomposition barrier. This result suggests that C−NO_2 bond scission is still a feasible reaction channel in TATB decomposition. Nevertheless, we will show in a later section that it is not the dominant one. The previously suggested N−O, N−H, and C−NH_2 bond scissions have barriers of at least 86.8, 96.3, and 103.4 kcal/mol, respectively. This led us to conclude that these pathways are not important processes in TATB decomposition.

C. Formation of Ions in C−NO_2 Bond Dissociation. In general, forming ions in the gas phase is an energetically disfavored reaction path due to its lack of screening of electronic charges. For instance, we found that it requires a large amount of energy, 208.8 kcal/mol, to form the ion pair during C−NO_2 bond breaking. The predicted reaction energies of TATB → $C_6H_6N_5O_4^+ + NO_2^-$ in the gas phase are listed in Table 3. It costs substantially more energy to ionize the $C_6H_6N_5O_4$ than the energy gain of forming NO_2^-. However, it is unknown whether ions form during the decomposition of solid TATB. We expect that inclusion of the dielectric effect in TATB solid will lower the energy, but not by a significant amount, since TATB is an insulator. Therefore, we believe that the ionization process is not important for solid TATB as well.

D. Carbon Ring Fission. The energetic cost to decompose TATB via the carbon ring fission pathway (shown in Figure 1f) was calculated using the same basis sets and DFT gradient-corrected functional (shown in Table 3). At the BPW91/Aug-cc-pVDZ level, its energy of reaction was calculated to be 185.8 kcal/mol, which sets the lower bound for its activation energy. It is not surprising that this process is energetically disfavorable since it involves breaking two carbon aromatic bonds. The large value suggests that this reaction path is not important in TATB thermal decomposition, which contradicts Farber and Srivastava's interpretation of their experiments.[18]

TABLE 4: DFT/BPW91 Transition State Barrier (E^{act}) and Reaction Energy (ΔE) of Intra- and Intermolecular Hydrogen Transfers (in kcal/mol)[a]

	intramolecular		intermolecular	
basis set	E^{act}	ΔE	ΔE (S)[b]	ΔE (D)[b]
D95V	46.8	45.6	72.4	67.3
cc-pVDZ	43.0	39.0	70.4	
Aug-cc-pVDZ	47.5	35.0	64.3	

[a] Values do not include zero-point energy. [b] S and D refer to single and double molecule calculation models, respectively.

E. Intra- and Intermolecular Hydrogen Transfers. In Figure 2a, we schematically show the intramolecular hydrogen transfer process. Table 4 lists the calculated transition state barrier(E^{act}) and energy of reaction (ΔE). We found the energy of reaction is 35.0 kcal/mol at the BPW91/Aug-cc-pVDZ level. Using the synchronous transit-guided quasi-Newton method, we located one transition state (TS) between TATB and the post-H-transfer biradical state (BR). TS was confirmed to have one imaginary frequency. We list the structure parameters of TS in Table 5, in which atom numbers are defined in Figure 2a. At the BPW91/Aug-cc-pVDZ level, TS gives a barrier height of 47.5 kcal/mol. The transition state geometry is close to BR, and is only 12.5 kcal/mol higher in energy than BR. This intramolecular hydrogen transfer has a barrier lower than that of the NO_2 bond breaking.

The intermolecular hydrogen transfer process is illustrated in Figure 2b, where a H atom of a TATB molecule moves to the next-nearest-neighbor oxygen atom of a nitro group of an adjacent TATB molecule. This process involves two TATB molecules. However, it is too computationally expensive to perform geometry optimizations using the double (D) TATB system. Therefore, we constructed the geometries of the initial and final states of the intermolecular H transfer by using the molecular structures optimized in the single (S) molecule model and placing the two molecules relative to each other according to the distance of TATB crystal X-ray data.[31] In the single-molecule model, each molecule is treated as an isolated gas phase species before and after the transfer. Therefore, it ignores the hydrogen bonding between two molecules and electronic coupling between two unpaired electrons. For the double molecule model, only a single point energy calculation was performed using the D95V basis set. We listed the energy of reactions (ΔE) obtained from both single and double molecule systems in Table 4. Interestingly the energy difference between ΔE from S and D model at the same basis set of D95V is 5.1 kcal/mol, which is about the strength of hydrogen bonding. If we assume the energy difference between the S and D models is also the same (5.1 kcal/mol) for the Aug-cc-pVDZ basis set, we estimate ΔE of D model/Aug-cc-pVDZ to be 59.2 kcal/mol based on the S model value of 64.3 kcal/mol.

Our best estimated energy of reaction gives a lower bound for the actual barrier of intermolecular hydrogen transfer. However, the calculated value of 59.2 kcal/mol is already higher than the barrier of 47.5 kcal/mol for intramolecular hydrogen transfer, which leads to the conclusion that intramolecular

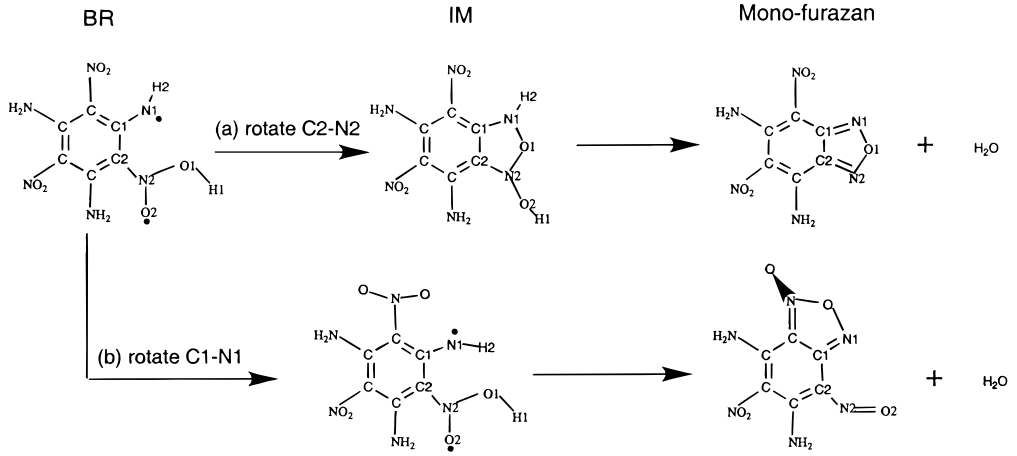

Figure 4. Possible mechanisms for the biradical to form (a) monobenzofurazan and (b) benzofuroxan-like compound.

TABLE 5: Bond Lengths (Å) and Angles (deg) for the Transition State (TS) of Intramolecular Hydrogen Transfer[a]

R(C1−N1) = 1.327	R(N1−H1) = 1.981	R(H1−O1) = 1.013	R(N1−H2) = 1.039
R(O1−N2) = 1.446	R(N2−C2) = 1.376	R(C1−C2) = 1.493	R(N2−O2) = 1.301
∠C1−N1−H1 = 107.1	∠N1−H1−O1 = 111.3	∠H1−O1−N2 = 105.8	∠O1−N2−C2 = 121.7
∠N2−C2−C1 = 120.3	∠C2−C1−N1 = 117.4	∠O1−N2−C2−C1 = −22.5	

[a] Atom numbers are defined in Figure 2a.

TABLE 6: DFT/BPW91 Reaction Energies (kcal/mol) for the Formation of Monobenzofurazan ($C_6H_4O_5N_6$), Bisbenzofurazan ($C_6H_2O_4N_6$), Trisbenzofurazan ($C_6O_3N_6$), and Benzofuroxan ($C_6H_4O_6N_6$)[a]

reaction/basis set	D95V	cc-pVDZ	Aug-cc-pVDZ
$C_6H_6O_6N_6 \rightarrow C_6H_4O_5N_6 + H_2O$	28.6	20.3	9.3(3.6)
$C_6H_4O_5N_6 \rightarrow C_6H_2O_4N_6 + H_2O$	23.0	14.3	6.5(1.7)
$C_6H_2O_4N_6 \rightarrow C_6O_3N_6 + H_2O$	19.3	10.7	3.5(1.1)
$C_6H_6O_6N_6 \rightarrow C_6H_4O_6N_6 + H_2$	67.3	59.4	58.2(48.3)

[a] See Figure 3 for reactions. Numbers in parentheses refer include the zero-point energy correction.

hydrogen transfer is the most energetically favored pathway. A possible explanation is that the coupling between the two unpaired electrons in the intramolecular mechanism provides additional stabilization of the transition state.

There is experimental evidence for the existence of free radicals in TATB. Britt et al. have reported that irradiation with ultraviolet (UV) light generates free radicals in TATB which are extremely stable (no decay after 2 years).[33] They used dimethyl sulfoxide or *N*,*N*-dimethylformamide to dissolve the free radical, which was suggested to be the H atom adduct of TATB based on their electron spin resonance data. However, they have noted that there is no evidence that the dissolved free radical is the same as the free radical in the solid (H-abstraction can occur from solvents, especially if some water is present). It is unknown whether the free radicals observed in their experiment has any relationship to the biradical involved in the hydrogen transfer reaction.

F. Formation of Benzofurazans via a Biradical. The predicted energies of reaction (ΔE) of benzofurazans were listed in Table 6 (reactions are defined in Figure 3). Increasing the size of the basis set significantly lowers the value of ΔE. The maximum deviation between values from D95V and Aug-cc-pVDZ is around 19 kcal/mol. However, note that the trend has been captured qualitatively by D95V. It has been suggested previously that the formations of bicyclic benzofurazan structures may be the first set of exothermic reactions. Our best estimates (BPW91/Aug-cc-pVDZ with zero-point energy correction) of ΔE for the formations of mono-benzofurazan (3,5 diamino-2,4 dinitrobenzofurazan), bisbenzofurazan (aminonitrobenzobisfurazan) and trisbenzofurazan (benzotrisfurazan) are slightly endothermic: 3.6, 1.7, and 1.1 kcal/mol, respectively.

TABLE 7: Reaction Energetics for the Conversion of Biradical (BR) Monobenzofurazan ($C_6H_4O_5N_6$) (Shown in Figure 4a)

reaction/basis set	D95V	cc-pVDZ	Aug-cc-pVDZ
BR → IM	3.5	15.3	12.8
IM → monobenzofurazan + H_2O	−20.5	−34.0	−38.4

There is limited experimental information regarding the details of forming benzofurazan derivatives. It is unknown whether the processes are unimolecular, bimolecular, or even trimolecular. One compound that has been suggested to be a potential intermediate species is benzofuroxan which has been observed in some subignited TATB samples. There is also the suggestion of benzofuroxan forming from TATB after losing H_2. The energy of reaction of this process is calculated and displayed in Table 6. At the BPW91/Aug-cc-pVDZ level, the reaction energy of the benzofuroxan pathway is 48.3 kcal/mol, with a large zero-point energy correction.

We propose that the biradical state, BR, is the precursor to benzofuroxan and benzofurazan derivatives. Figure 4, a and b, shows two possible paths from which BR turns into benzofurazan and benzofuroxan like species, respectively. In path a, BR first undergoes a C2−N2 single-bond rotation which typically has a barrier of roughly a few kcal/mol. This rotation brings the two unpaired electrons in the same bonding region such that a new bond between N1 and O1 can be formed easily. We found that the energy of this intermediate state (IM) is only 12.8 kcal/mol (shown in Table 7, at the BPW91/Aug-cc-pVDZ level) higher than that of the BR state. When IM loses H_2O, monobenzofurazan forms which releases a significant amount of energy, 38.4 kcal/mol. In path b, BR first rotates C1−N1 bond instead. Then, the unpaired electron at N1 attacks the nearby O atom. At the same time, H2 attacks O1−H1 group to form water. This process creates benzofuroxan-like species.

The mechanism of intramolecular hydrogen transfer → BR → benzofurazan derivatives is consistent with several (but not all) experimental observations which are otherwise conflicting under other proposed decomposition models. For instance, it is

consistent with experiments that observed the reduction of NH_2 and NO_2 groups.[9−13,16] In addition, it is also consistent with isotopic kinetics data which requires motion of hydrogen.[7]

IV. Summary

Push−pull benzene ring molecules, such as TATB, have a variety of competing intramolecular and intermolecular decomposition pathways. Using first-principles density functional theory, we conducted a comprehensive study of the reaction energetics of gas phase TATB which includes eight pathways. Among them, five reaction paths (breaking of N−H, N−O, and C−NH_2 bonds, formations of NO_2^{-1} and carbon-ring fission) were found to have energy more than 40 kcal/mol above the minimum energy pathway; therefore, we characterize them as rare events. The intermolecular hydrogen transfer was found to have a barrier of >59.2 kcal/mol, which is at least 11.7 kcal/mol (∼6000 K) higher than that of intramolecular hydrogen transfer. However, we do not know its actual barrier to determine whether it is a weak path or a rare event. In addition, our result is based on the intermolecular distance of the uncompressed TATB, and therefore it does not apply to situations (e.g., shock) where TATB has a shorter intermolecular separation than that at ambient pressure.

We found that the intramolecular hydrogen transfer process has the lowest activation barrier of 47.5 kcal/mol, which forms a biradical precursor state of benzofuroxan and benzofurazan derivatives.[9] This new mechanism is in agreement with the hydrogen isotope experiments[7] and the reports of benzofuroxan and benzofurazan-like spectra.[11] It also is consistent with the experiments that observed loss of NO_2 group[11] and drop of IR intensity of C−NH_2 bond stretching.[16] Another pathway that has a barrier in the vicinity of the overall barrier of decomposition is unimolecular NO_2 bond dissociation. Our calculations indicate that this pathway should play a minor role, since its barrier is 16.4 kcal/mol (∼8000 K) higher than that of intramolecular hydrogen transfer.

We have shown in this work that hydrogen bonding not only plays a role in determining the structure of TATB, but also in its chemistry. The ring closure mechanism is found to be mediated by the intramolecular hydrogen transfer and to compete directly with simple C−NO_2 bond breaking. Such a mechanism is expected to apply to other related materials such as nitroaniline (1-amino-2-nitrobenzene) and DATB (1,3-diamino-2,4,6-trinitrobenzene).

Acknowledgment. We thank Dr. L. L. Yan for her insightful suggestions. We also thank Dr. M. R. Manaa and Dr. C. Tarver for useful comments made during the preparation of the manuscript. This work was performed under the auspices of the U.S. Department of Energy by the Lawrence Livermore National Laboratory under contract No. W-7405-ENG-48.

References and Notes

(1) Baldridge, K. K.; Siegel, J. S. *J. Am. Chem. Soc.* **1993**, *115*, 10782.

(2) Fields, E. K.; Meyerson, S. *J. Am. Chem. Soc.* **1967**, *89*, 724.

(3) Politzer, P.; Abrahmsen, L.; Sjoberg, P. *J. Am. Chem. Soc.* **1984**, *106*, 855.

(4) Rice, S. F.; Simpson, R. L. "The Unusual Stability of TATB: A Review of The Scientific Literature"; LLNL Report, UCRL-LR-103683.

(5) Stolovy, A.; Jones, E. C., Jr.; Aviles, J. B.; Namenson, A. I.; Fraser, W. A. *J. Chem. Phys.* **1983**, *78*, 229.

(6) Catalano, E.; Crawford, P. C. *Thermochim. Acta* **1983**, *61*, 23.

(7) Rogers, R. N.; Janney, J. L.; Ebinger, M. H. *Thermochim. Acta* **1982**, *59*, 287.

(8) Brill, T. B.; James, K. J. *J. Phys. Chem.* **1993**, *97*, 8752.

(9) Sharma, J.; Owens, F. J. *Chem. Phys. Lett.* **1979**, *61*, 280.

(10) Sharma, J.; Garrett, W. L.; Owens, F. J.; Vogel, V. L. *J. Phys. Chem.* **1982**, *86*, 1657.

(11) Sharma, J.; Hoffsommer, J. C.; Glover, D. J.; Coffey, C. S.; Santiago, F.; Stolovy, A.; Yasuda, S. *Shock Waves in Condens. Matter*; Asay, J. R., Graham, R. A., Straub, G. K., Eds.; Elsevier Science Publishers: Amsterdam, 1984; p 543.

(12) Sharma, J.; Forbes, J. W.; Coffey, C. S.; Liddiard, T. P. *J. Phys. Chem.* **1987**, *91*, 5139.

(13) Land, T. A.; Siekhaus, W. J.; Foltz, M. F.; Behrens, R., Jr. *Proc. 10th Symp. (Int.) Detonation, Boston, MA, July 12−16, 1993*; ONR 33395-12, 1995; p 181.

(14) Catalano, E.; Rolon, C. E. *Thermochim. Acta* **1983**, *61*, 53.

(15) Catalano, E.; Rolon, C. E. *Thermochim. Acta* **1983**, *61*, 37.

(16) Makashir, P. S.; Kurian, E. M. *J. Thermal Anal.* **1996**, *46*, 225.

(17) Ostmark, H. In *Shock Compression of Condens. Matter−1995*; AIP: New York, 1996; p 871.

(18) Farber, M.; Srivastava, R. D. *Combust. Flame* **1981**, *42*, 165.

(19) Davis, L. L.; Brower, K. R. In *Shock Compression of Condens. Matter−1997*; Schmidt, S. C., Dandekar, D. P., Forbes, J. W., Eds.; AIP: New York, 1998; p 699.

(20) Minier, L. M.; Brower, K. R.; Oxley, J. C. *J. Org. Chem.* **1991**, *56*, 3306.

(21) Becke, A. D. *J. Chem. Phys.* **1992**, *97*, 9173.

(22) Johnson, B. G.; Gill, P. M. W.; Pople, J. A. *J. Chem. Phys.* **1993**, *98*, 5612.

(23) Durant, J. L. *Chem. Phys. Lett.* **1996**, *256*, 595.

(24) Frisch, M. J.; Trucks, G. W.; Schlegel, H. B.; Gill, P. M. W.; Johnson, B. G.; Robb, M. A.; Cheeseman, J. R.; Keith, T. A.; Petersson, G. A.; Montgomery, J. A.; Raghavachari, K.; Al-Laham, M. A.; Zakrzewski, V. G.; Ortiz, J. V.; Foresman, J. B.; Cioslowski, J.; Stefanov, B. B.; Nanayakkara, A.; Challacombe, M.; Peng, C. Y.; Ayala, P. Y.; Chen, W.; Wong, M. W.; Andres, J. L.; Replogle, E. S.; Gomperts, R.; Martin, R. L.; Fox, D. J.; Binkley, J. S.; Defrees, D. J.; Baker, J.; Stewart, J. P.; Head-Gordon, M.; Gonzalez, C.; Pople, J. A. *Gaussian 94*; Gaussian, Inc.: Pittsburgh, PA, 1995.

(25) Kohn, W.; Sham, L. *Phys. Rev. A* **1965**, *140*, 1133.

(26) Becke, A. D. *Phys. Rev. A* **1988**, *38*, 3098.

(27) Perdew, J. P.; Wang, Y. *Phys. Rev. B* **1992**, *45*, 13244.

(28) Wu, C. J.; Fried, L. E. *J. Phys. Chem.* **1997**, *101*, 8675.

(29) Dunning, T. H., Jr.; Hay, P. J. *Modern Theoretical Chemistry*; Plenum: New York, 1976.

(30) Dunning, T. H., Jr. *J. Chem. Phys.* **1989**, *90*, 1007.

(31) Cady, H. H.; Larson, A. C. *Acta Crystallogr.* **1965**, *18*, 485.

(32) Wu, C. J., et al., to be published.

(33) Britt, A. D.; Moniz, W. B.; Chingas, G. C.; Moore, D. W.; Heller, C. A.; Ko, C. L. *Propellants, Explos. Pryrotech.* **1981**, *6*, 94.